Molecular Neurobiology (2019) 56:6035–6045
https://doi.org/10.1007/s12035-019-1505-6

Prions Strongly Reduce NMDA Receptor S-Nitrosylation Levels at Pre-symptomatic and Terminal Stages of Prion Diseases

Elisa Meneghetti[1] · Lisa Gasperini[1] · Tommaso Virgilio[2] · Fabio Moda[2] · Fabrizio Tagliavini[3] · Federico Benetti[1,4] · Giuseppe Legname[1,5]

Received: 15 October 2018 / Accepted: 23 January 2019 / Published online: 1 February 2019

Abstract

Prion diseases are fatal neurodegenerative disorders characterized by the cellular prion protein (PrP^{C}) conversion into a misfolded and infectious isoform termed prion or PrP^{Sc}. The neuropathological mechanism underlying prion toxicity is still unclear, and the debate on prion protein gain- or loss-of-function is still open. PrP^{C} participates to a plethora of physiological mechanisms. For instance, PrP^{C} and copper cooperatively modulate *N*-methyl-D-aspartate receptor (NMDAR) activity by mediating S-nitrosylation, an inhibitory post-translational modification, hence protecting neurons from excitotoxicity. Here, NMDAR S-nitrosylation levels were biochemically investigated at pre- and post-symptomatic stages of mice intracerebrally inoculated with RML, 139A, and ME7 prion strains. Neuropathological aspects of prion disease were studied by histological analysis and proteinase K digestion. We report that hippocampal NMDAR S-nitrosylation is greatly reduced in all three prion strain infections in both pre-symptomatic and terminal stages of mouse disease. Indeed, we show that NMDAR S-nitrosylation dysregulation affecting prion-inoculated animals precedes the appearance of clinical signs of disease and visible neuropathological changes, such as PrP^{Sc} accumulation and deposition. The pre-symptomatic reduction of NMDAR S-nitrosylation in prion-infected mice may be a possible cause of neuronal death in prion pathology, and it might contribute to the pathology progression opening new therapeutic strategies against prion disorders.

Keywords Prions · NMDA receptor · S-Nitrosylation · Nitric oxide · Copper · Excitotoxicity

Introduction

Prion diseases are a group of rare, rapidly progressive and fatal neurodegenerative pathologies affecting both humans and animals [1, 2]. The causative agent of prion diseases is the scrapie prion protein (PrP^{Sc}, or prion), derived from a conformational conversion of the cellular prion protein (PrP^{C}) into a β-sheet enriched isoform [3–6]. Prions can recruit PrP^{C}

Electronic supplementary material The online version of this article (https://doi.org/10.1007/s12035-019-1505-6) contains supplementary material, which is available to authorized users.

✉ Giuseppe Legname
legname@sissa.it

Elisa Meneghetti
emene@sissa.it

Lisa Gasperini
lisa.gasperini@gmail.com

Tommaso Virgilio
Tommaso.Virgilio@istituto-besta.it

Fabio Moda
Fabio.Moda@istituto-besta.it

Fabrizio Tagliavini
Fabrizio.Tagliavini@istituto-besta.it

Federico Benetti
f.benetti@ecamricert.com

[1] Laboratory of Prion Biology, Department of Neuroscience, Scuola Internazionale Superiore di Studi Avanzati (SISSA), Trieste, Italy

[2] Fondazione IRCCS Istituto Neurologico Carlo Besta, Unit of Neuropathology and Neurology-5, Milano, Italy

[3] Fondazione IRCCS Istituto Neurologico Carlo Besta, Scientific Directorate, Milano, Italy

[4] ECSIN-European Center for the Sustainable Impact of Nanotechnology, ECAMRICERT SRL, Padova, Italy

[5] ELETTRA Laboratory, Sincrotrone Trieste S.C.p.A., Basovizza, Trieste, Italy

molecules and force their conversion into misfolded isoforms, which are more prone to aggregation [7, 8]. The deposition of prion aggregates is a neuropathological feature of the disease, together with brain gliosis, spongiform degeneration, and neuronal loss [9, 10].

The mechanism underlying prion neurotoxicity has been largely debated, and both a gain of toxic function for PrP^{Sc} and a loss of function for PrP^{C} have been proposed [11–13]. Therefore, to fully understand prion pathologies, a clear definition of PrP^{C} function is of utmost importance [14, 15].

One of the most intriguing roles of PrP^{C} consists in the protection of neurons from excitotoxicity, by modulating glutamatergic synapses and preventing excessive calcium influx [16–29]. In particular, PrP^{C} inhibits *N*-methyl-D-aspartate receptors (NMDARs) in a copper (Cu)-dependent manner [26, 27]. In our previous work, we showed that PrP^{C} modulates NMDARs by promoting S-nitrosylation, a post-translational modification consisting in the covalent attachment of nitric oxide (NO) to a cysteine thiol group [30–33]. This reaction is supported by NO, produced by nitric oxide synthase (NOS) [31, 34, 35], and PrP^{C}-bound Cu(II). In the synaptic cleft, PrP^{C} is localized in lipid raft domains in close proximity to NMDARs [36, 37]: here, PrP^{C} binds Cu and sustains its redox cycling [38–42]. PrP^{C}-bound Cu(II) acts as electron acceptor by being reduced to Cu(I), thus allowing NO oxidation and subsequent S-nitrosylation of GluN2A and GluN1 receptor subunits. S-Nitrosylation determines NMDAR desensitization and prevents NMDAR-coupled ionic channel over-activation [30–32]. Consequently, PrP^{C} knockout mice lack this neuroprotective mechanism and present an increased susceptibility to excitotoxicity [30].

In the present study, we analyzed the levels of NMDAR S-nitrosylation in prion-infected mice. By using hippocampal samples isolated from mice infected with three different prion strains, we evaluated GluN2A and GluN1 S-nitrosylation levels at both terminal and pre-symptomatic stages of the disease and compared with those in age-matched control mice. In prion-infected mice, we found a reduction of NMDAR S-nitrosylation level at both terminal and pre-symptomatic stages, suggesting an early loss of PrP^{C} protective function. Therefore, the impairment of NMDAR S-nitrosylation may be one of the mechanisms causing neuronal cell toxicity in prion pathology.

Results

Characterization of Prion Disease in Intracerebrally Inoculated Mice at Pre-symptomatic and Terminal Stage

Before investigating the effect of prion infection on NMDAR S-nitrosylation levels, we characterized biochemical and neuropathological aspects of prion disease in the mouse models we used. Brain samples of CD1 female mice intracerebrally inoculated with three different mouse-adapted scrapie strains RML, 139A, and ME7 were collected 30 days post-infection (dpi), considered as pre-symptomatic stage, and at the terminal stage of the disease, corresponding to 150.2 ± 5.1, 154.7 ± 7.1, and 160.3 ± 8.7 dpi (± standard deviation, SD), respectively. In the present study, we focused our attention on the hippocampus, since PrP^{C} is strongly expressed in this brain structure [43] and since this region is rich in glutamatergic synapses [44].

Limited resistance to proteolysis is a diagnostic method for PrP^{Sc} detection [4, 45]. Therefore, we treated hippocampal homogenates from control and infected samples at pre-symptomatic and terminal stages with proteinase K (PK) and detected PK-resistant fragments by Western blotting. For all three prion strains analyzed, we observed no PK-resistance at pre-symptomatic phase of the disease (Fig. 1a). Conversely, all samples of terminally diseased mice presented PK-resistant fragments, with 139A prion strain showing a milder accumulation of PrP^{Sc} compared with the other two strains (Fig. 1b).

To verify the amount and distribution of PrP^{Sc} deposits, we performed immunohistochemistry analysis of hippocampal regions [10] (Fig. 2a–f). While no PrP^{Sc} was found in the hippocampus of mice sacrificed at pre-clinical stage of the disease (Fig. 2a–c), all the animals culled at terminal stage were severely affected by PrP^{Sc} accumulation (Fig. 2d–f). Regardless of the strain, a prevalent synaptic and diffuse pattern of deposition was detected. Differences were mainly confined to the region where hippocampal neurons receive direct input from the enthorinal cortex, named *stratum lacunosum-moleculare*, which was most affected in RML-injected animals (Fig. 2d), and to the presence of plaque-like deposits in the hippocampus of ME7-injected mice (Fig. 2f).

To verify the presence of spongiosis, we performed hematoxylin and eosin (H&E) staining (Fig. 2g–l). As expected, spongiform changes were present in all hippocampi of terminally ill mice (Fig. 2j–l) but were considerably more severe in ME7-injected mice than in RML or 139A-infected animals.

NMDAR S-Nitrosylation Is Reduced at the Terminal Stage of Prion Diseases

While in healthy conditions PrP^{C} and Cu cooperatively protect neurons by modulating NMDAR activity through the S-nitrosylation [30], in prion diseases loss of PrP^{C} protective function, due to its conversion into PrP^{Sc}, might reduce NMDAR S-nitrosylation levels. To test this hypothesis, we measured GluN2A and GluN1 S-nitrosylation levels in hippocampi isolated from mice infected with either RML, 139A, or ME7 prion strain at the terminal stage and compared them with those of age-matched controls. We evaluated S-nitrosylation levels by using two distinct methods: the biotin switch assay and the SNOB1 assay. Western blotting signals

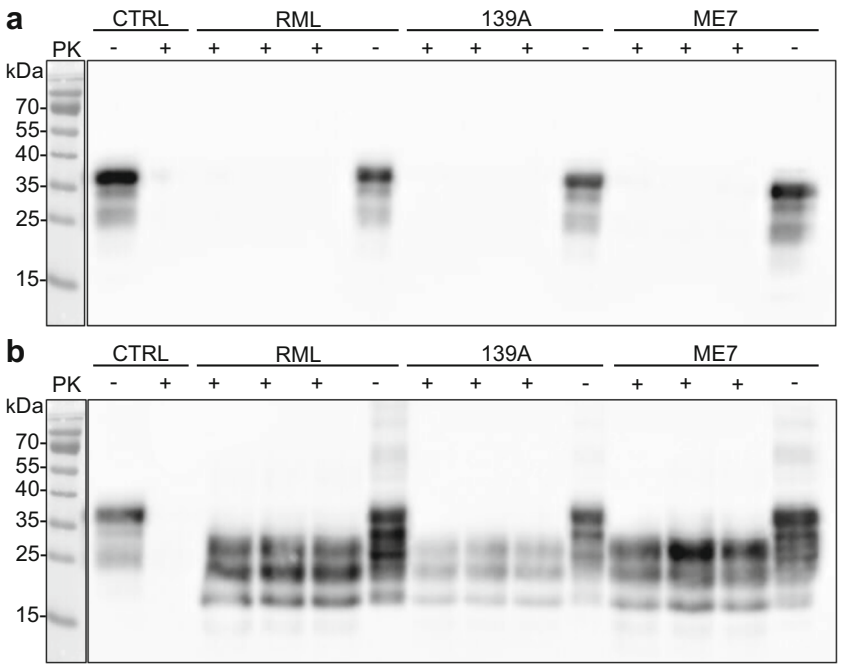

Fig. 1 PK-resistant fragments of PrP are detected in terminally ill, but not in pre-symptomatic mice. Western blot of hippocampal proteins from infected samples and from age-matched controls, digested (+) or not (−) with PK. **a** Pre-symptomatic stage of prion disease. **b** Terminal stage of prion disease. Molecular weights are stated on the left-hand side (kDa)

corresponding to S-nitrosylated proteins—GluN2A, GluN1, and β-actin—were normalized against their respective input signals. The resulting GluN2A and GluN1 ratio values were normalized versus β-actin ratio value, and data from terminally ill and control animals were compared by Student's *t* test.

In the hippocampus of RML-terminal mice, with biotin switch assay we detected lower GluN2A ($n = 3$, $p = 0.0082$) and GluN1 ($n = 3$, $p = 0.0216$) S-nitrosylation levels compared with those of age-matched controls (Fig. 3a). Similar observations were obtained by using SNOB1 assay (GluN2A, $n = 3$, $p = 0.0019$; GluN1, $n = 3$, $p = 0.0362$) (Fig. 4a and

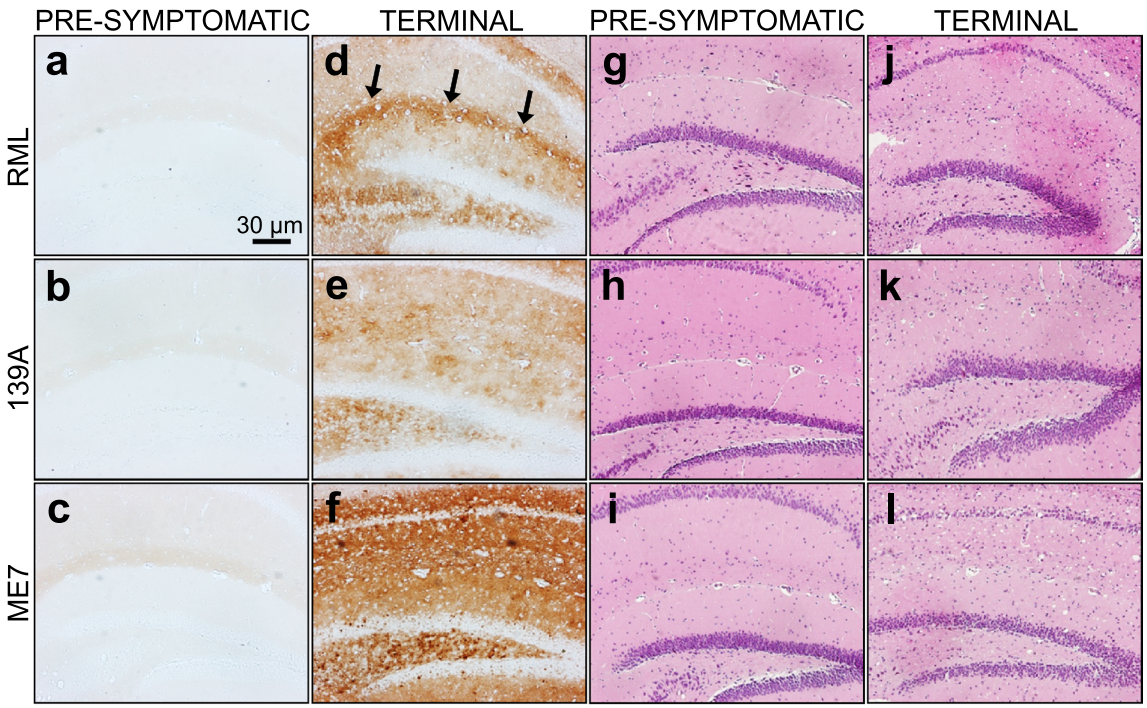

Fig. 2 Histological characterization of prion disease mice at pre-symptomatic and terminal stage. **a**–**f** PrP^{Sc} immunohistochemistry in the hippocampus of prion disease mice at pre-symptomatic and terminal stage. **g**–**l** H&E staining for the visualization of spongiform changes in prion disease mice at pre-symptomatic and terminal stage. Arrows indicate the *stratum lacunosum-moleculare* of the hippocampus. Scale bar corresponds to 30 µm

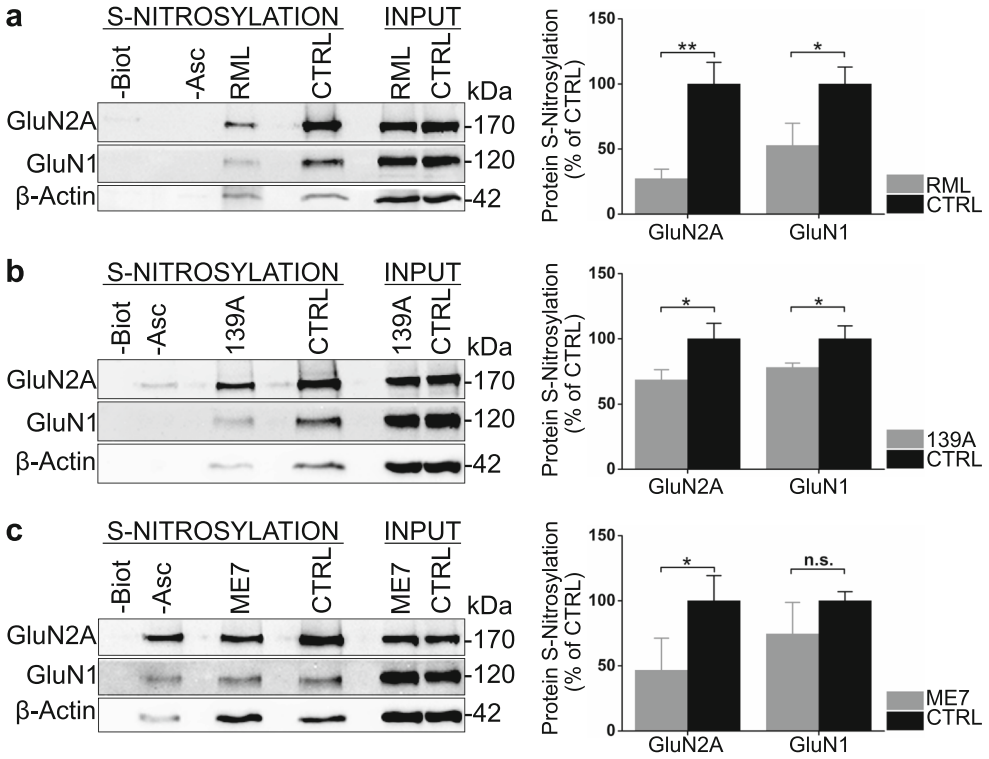

Fig. 3 S-Nitrosylation of NMDAR subunits in hippocampi of control and terminally infected mice detected by biotin switch assay. On the left side: representative images of S-nitrosylated fractions, controls without either biotin (− Biot) or ascorbate (− Asc), and corresponding input of GluN2A, GluN1, and β-actin. Controls without either biotin or ascorbate were done using non-infected samples. On the right side: graphs showing the quantification of S-nitrosylated GluN2A and GluN1 immunoblot signals in infected mice expressed as percentage of the control values. Experiments were performed in hippocampi of RML ($n = 3$ experiments) (**a**), 139A ($n = 3$ experiments) (**b**), and ME7 ($n = 3$ experiments) (**c**) infected mice at terminal stage of disease. All error bars indicate SD; $^{*}p < 0.05$; $^{**}p < 0.01$; *n.s.* not significant

Supplementary Fig. S1). Similar to RML-infected mice, our results from 139A-terminal mouse hippocampi tested in the biotin switch assay showed reduced GluN2A ($n = 3$, $p = 0.0239$) and GluN1 ($n = 3$, $p = 0.0493$) S-nitrosylation levels (Fig. 3b). Although not statistically significant because of low sample size available, we also reported a 60% reduction of NMDAR S-nitrosylation by SNOB1 assay (Fig. 4b and Supplementary Fig. S2). Finally, data obtained from ME7-terminal mice confirmed what has been observed in RML- and 139A-infected samples. Indeed, we described a reduction in GluN2A (biotin switch assay, $n = 3$, $p = 0.0446$; SNOB1, $n = 3$, $p = 0.0842$) (Figs. 3c and 4c) and in GluN1 S-nitrosylation levels (biotin switch assay, $n = 4$, $p = 0.1231$; SNOB1 assay, $n = 3$, $p = 0.0039$) (Figs. 3c and 4c and Supplementary Fig. S3).

These findings clearly revealed that at the terminal stage of prion infection, hippocampal NMDAR S-nitrosylation levels are strongly reduced.

NMDAR S-Nitrosylation Is Reduced at Pre-symptomatic Stage of Prion Diseases

To define if alterations in NMDAR S-nitrosylation constitute an early event in the progression of prion diseases, we analyzed GluN2A and GluN1 S-nitrosylation levels in the hippocampus of mice infected with either RML or 139A or ME7 prion strain at the pre-symptomatic stage, i.e., 30 dpi.

RML-infected hippocampi tested in the biotin switch assay presented a reduced GluN2A ($n = 4$, $p = 0.0205$) and GluN1 ($n = 4$, $p = 0.0057$) S-nitrosylation level compared with age-matched controls (Fig. 5a). These results were also confirmed by using SNOB1 assay (GluN2A, $n = 4$, $p = 0.0076$; GluN1, $n = 4$, $p = 0.0322$) (Fig. 6a and Supplementary Fig. S4). In 139A-infected animals, S-nitrosylation reduction was observed for both NMDAR subunits with biotin switch assay (GluN2A, $n = 4$, $p = 0.0160$; GluN1, $n = 4$, $p = 0.0381$) and SNOB1 assay (GluN2A, $n = 3$, $p = 0.0234$; GluN1, $n = 4$, $p = 0.0170$) (Figs. 5b and 6b and Supplementary Fig. S5).

The pre-symptomatic ME7-infected animals were characterized by lower S-nitrosylation levels of GluN2A ($n = 4$, $p = 0.0018$) and GluN1 ($n = 4$, $p = 0.0500$) than healthy age-matched animals (Fig. 5c, biotin switch assay). By using SNOB1 assay, a 15% reduction in S-nitrosylation levels of both NMDAR subunits was measured, though not statistically evaluable due to the single sample employed (Fig. 6c and Supplementary Fig. S6).

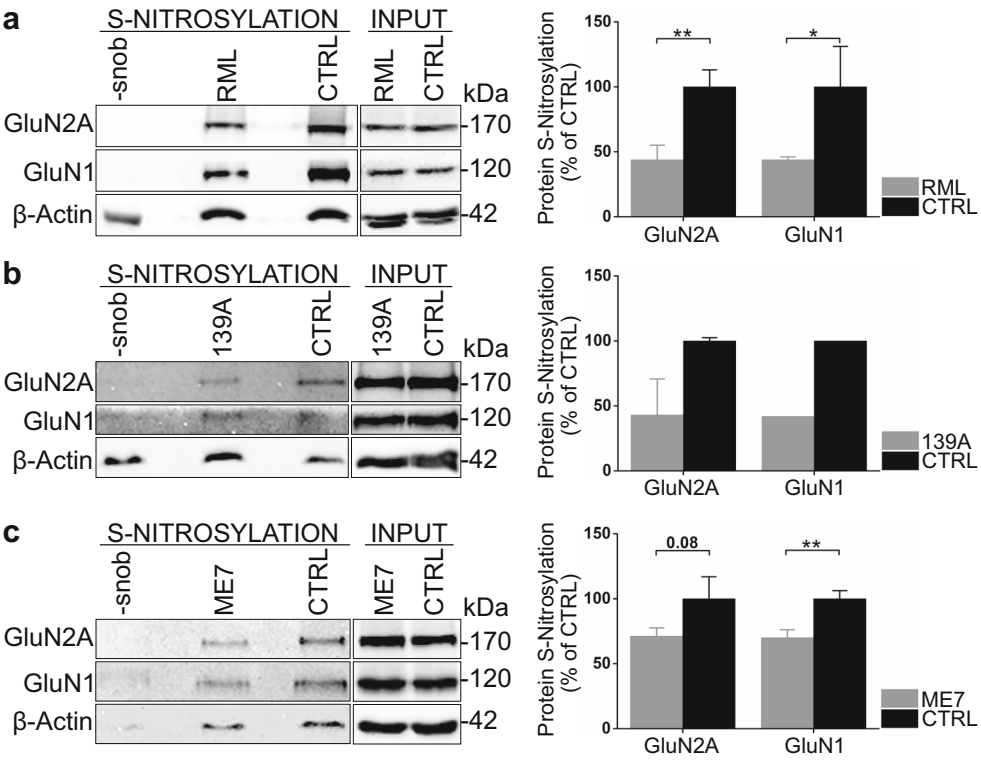

Fig. 4 S-Nitrosylation of NMDAR subunits in hippocampi of control and terminally infected mice, measured by SNOB1 assay. On the left side: cropped representative images of immunoblot signals corresponding to SNOB1-bound GluN2A, GluN1, and β-actin in control and terminally ill mice infected with RML ($n = 3$ experiments) (**a**), 139A ($n = 2$ experiments) (**b**), and ME7 ($n = 3$ experiments) (**c**) prion strain. Controls without SNOB (− snob) were done using control samples. Uncropped images are available in Supplementary Figs. 1–3. On the right side: graphs showing the quantification of S-nitrosylation immunoblot signals in prion-infected mice represented as percentage of the control values. All error bars indicate SD; $*p < 0.05$; $**p < 0.01$

These results show a reduction in NMDAR S-nitrosylation levels also at the pre-symptomatic stage of prion diseases, when the presence of PrP^{Sc} is not yet detectable by biochemical and histological methods.

Discussion

A comprehensive definition of PrP^{C} physiological activity is crucial, since its alterations may represent a pathological

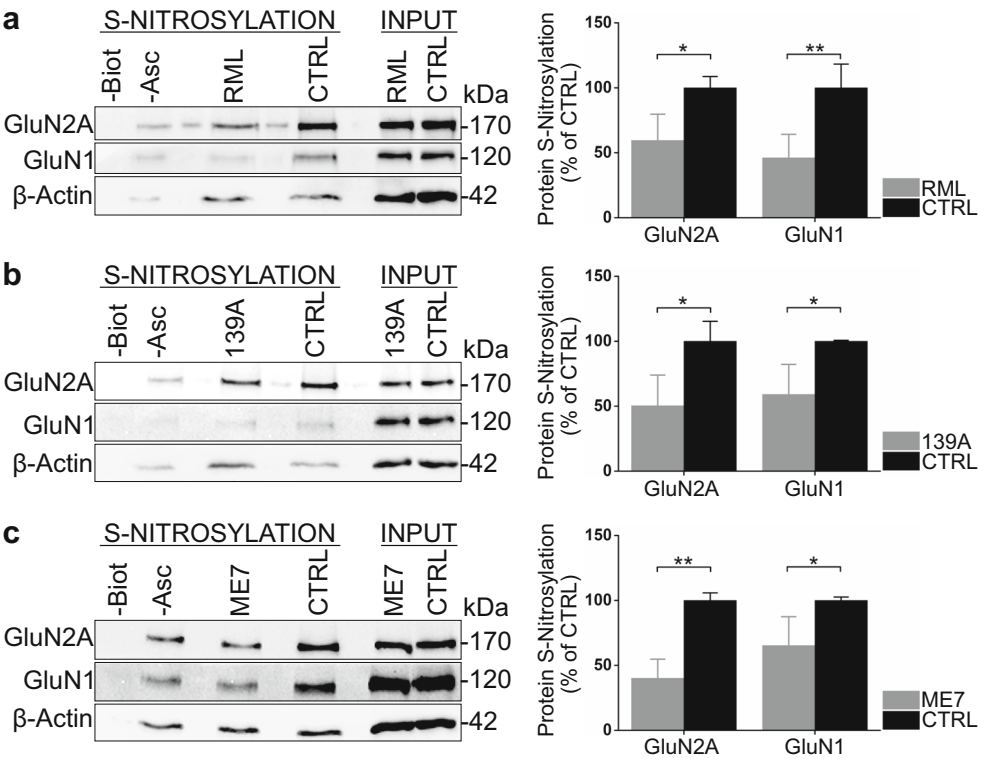

Fig. 5 S-Nitrosylation of NMDAR subunits in hippocampi of control and pre-symptomatic prion-infected mice detected by biotin switch assay. On the left side: representative images of S-nitrosylated fractions, controls without either biotin (− Biot) or ascorbate (− Asc), and corresponding input of GluN2A, GluN1, and β-actin. Controls without either biotin or ascorbate were done using non-infected samples. On the right side: graphs showing the quantification of S-nitrosylated GluN2A and GluN1 immunoblot signals in infected mice expressed as percentage of the control values. Experiments were performed in hippocampi of RML ($n = 4$ experiments) (**a**), 139A ($n = 4$ experiments) (**b**), and ME7 ($n = 4$ experiments) (**c**) infected mice at pre-symptomatic stage of disease. All error bars indicate SD; $*p < 0.05$; $**p < 0.01$

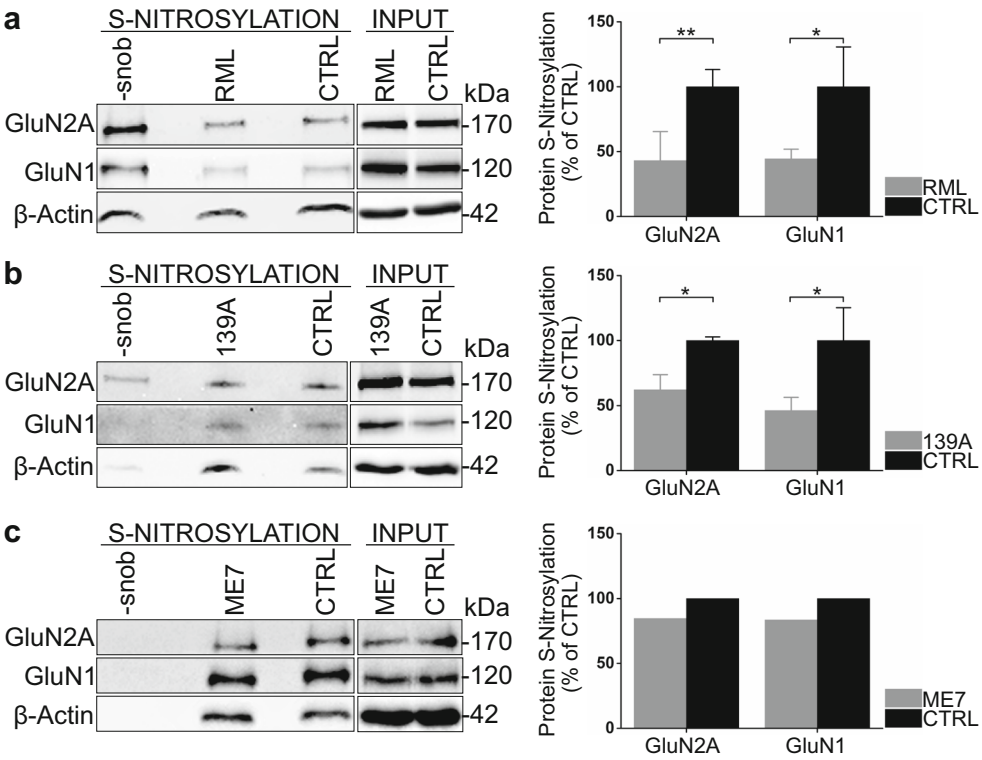

Fig. 6 S-Nitrosylation of NMDAR subunits in hippocampi of control and pre-symptomatic prion-infected mice measured by SNOB1 assay. On the left side: cropped representative images of immunoblot signals corresponding to SNOB1-bound GluN2A, GluN1, and β-actin in control and pre-symptomatic mice infected with RML ($n = 4$ experiments) (**a**), 139A ($n = 3$ experiments) (**b**), and ME7 ($n = 1$ experiments) (**c**) prion strain. Controls without SNOB (− snob) were done using control samples. Uncropped images are available in Supplementary Figs. 4–6. On the right side: graphs showing the quantification of S-nitrosylation immunoblot signals in prion-infected mice represented as percentage of the control values. All error bars indicate SD; $*p < 0.05$; $**p < 0.01$

mechanism in prion diseases [46]. Although PrP^C genetic ablation, both prenatally [47, 48] and post-natally [21], does not trigger gross disturbances in mice, upon deeper analysis many subtle phenotypic changes have been reported. Indeed, PrP^C has been implicated in a plethora of physiological processes with defined mechanisms of action [11, 14, 15, 49–51].

In a previous work, we described the neuroprotective mechanism based on NMDAR inhibition through S-nitrosylation and mediated by PrP^C, Cu, and NO [30]. At glutamatergic synapses, PrP^C-bound Cu(II) can be reduced to Cu(I) to support NO oxidation [38] and the ensuing NO^+ electrophilic attack to GluN2A and GluN1 extracellular cysteine thiols, resulting in NMDAR S-nitrosylation [31]. S-Nitrosylation induces the receptor desensitization and prevents the NMDAR-coupled ionic channel over-activation in stressful conditions (Fig. 7a) [32].

As prion diseases, similar to other neurodegenerative disorders, show alterations at the level of glutamatergic synapses and increased susceptibility to excitotoxicity [52], we hypothesized that the loss of PrP^C-mediated neuroprotection through NMDAR S-nitrosylation could be implied in the pathology progression. Our results confirmed that NMDAR S-nitrosylation is impaired in mouse models of prion disease. By comparing GluN2A and GluN1 S-nitrosylation levels in prion-infected mouse hippocampi with those in controls, we found a reduction of NMDAR S-nitrosylation at both terminal and pre-symptomatic stages of the disease, when the amount of PrP^C to PrP^{Sc} conversion was still not biochemically detectable. We confirmed our results by inoculating mice with different prion strains that develop different disease features, such as neuropathological lesion profile, biochemical properties, and PrP^{Sc} deposition pattern in the brain [53, 54].

Since a similar phenotype occurs in PrP^C knockout models [30], NMDAR S-nitrosylation decrease in prion-infected mice is likely caused by loss of PrP^C function.

The mechanism underlying prion damage has been largely debated. Given its accumulation in the brain and ability to transmit fatal neurodegeneration [55–57], PrP^{Sc} was initially considered to be the neurotoxic species. However, many lines of evidence show that PrP^{Sc} itself is not sufficient for the disease progression and point to a central role of PrP^C loss of biological activity [12, 58, 59]. Our results suggest a combination of gain- and loss-of-function mechanisms to explain prion pathology: while the loss of PrP^C biological activity is not sufficient to induce neurodegeneration, NMDAR S-nitrosylation reduction enhances the susceptibility to excitotoxicity, leading to cell death in the presence of stressful conditions caused by PrP^{Sc} accumulation.

Different hypotheses may explain the impairment of NMDAR S-nitrosylation in prion-infected mouse hippocampus [11]. First, the biological activity of PrP^C might be lost upon contact or binding to PrP^{Sc}, blocking some functional domains of the protein, such as the N-terminal flexible region binding Cu ions (Fig. 7b) [60–62]. Secondly, Cu sequestration by PrP^{Sc} aggregates may reduce Cu availability in the synaptic cleft, thus limiting NO oxidation and ensuing cysteine S-nitrosylation (Fig. 7c) [63, 64]. Moreover, the impaired NMDAR S-nitrosylation in prion-infected mice could be due

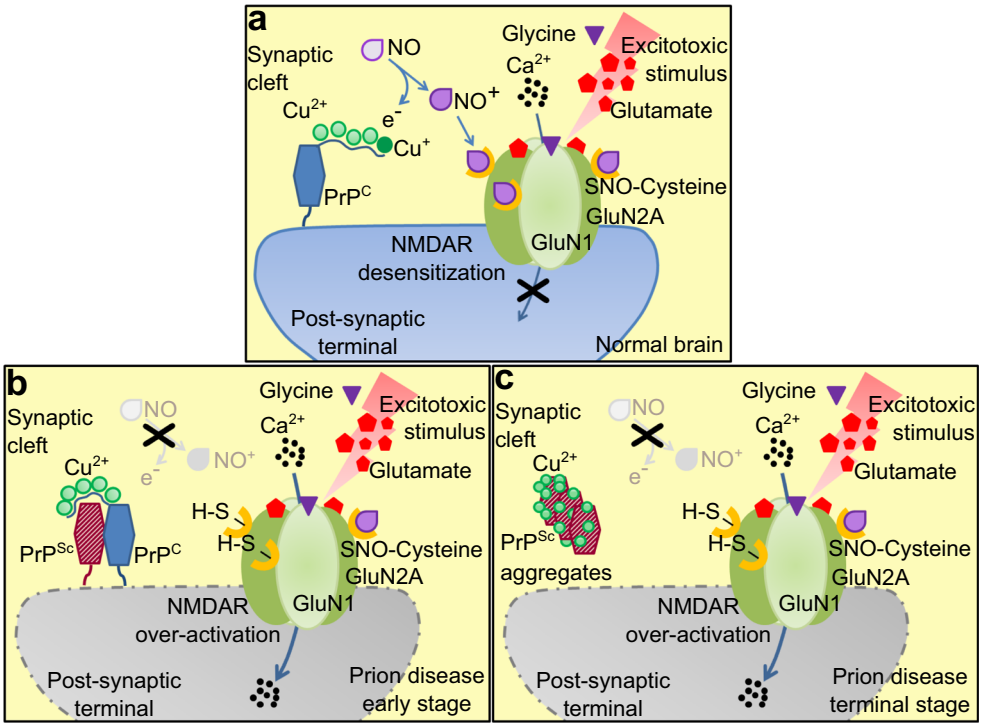

Fig. 7 Neuroprotective NMDAR inhibition through PrP^C-mediated S-nitrosylation is impaired in prion disease. **a** In normal brains at glutamatergic synapses, PrP^C-bound Cu(II) can be reduced to Cu(I) to support NO oxidation and the ensuing S-nitrosylation of cysteine residues on GluN2A and GluN1 NMDAR subunits. In the presence of excitotoxic stimuli, S-nitrosylation induces NMDAR desensitization and prevents the NMDAR-coupled ionic channel over-activation, avoiding excitotoxicity. **b**–**c** In prion disease, loss of PrP^C-mediated neuroprotection through NMDAR S-nitrosylation enhances the susceptibility to excitotoxicity, leading to cell death in the presence of stressful conditions. During early stage of prion disease, the biological activity of PrP^C might be lost upon contact or binding to PrP^{Sc}, blocking some functional domains of the protein, such as the N-terminal flexible region binding Cu ions (**b**). At terminal stage of prion disease, PrP^{Sc} aggregates may sequester Cu, reducing its availability in the synaptic cleft, thus limiting NO oxidation and ensuing cysteine S-nitrosylation (**c**)

to differences in NMDAR and/or NOS expression. While we did not observe any decrease in NMDAR expression during prion disease progression, evidence reported in literature shows an increase in brain NO level, NOS expression, and NOS activity [65, 66]. Therefore, NOS/NO pathway is unlikely to be the limiting factor that impedes the proper NMDAR S-nitrosylation.

In this study, we point out that the reduction of NMDAR S-nitrosylation in prion-infected mice precedes the appearance of clinical signs of disease and of visible neuropathological changes, such as PrP^{Sc} accumulation, aggregation, formation of plaque-like deposits, and spongiosis. Therefore, dysregulation of NMDAR S-nitrosylation may be considered a possible cause of neuronal death in prion pathology.

The finding of decreased NMDAR S-nitrosylation in prion-infected mouse hippocampus opens the possibility for a new therapeutic approach against prion disorders. At present, most therapeutic strategies are aimed at inhibiting PrP^{Sc} conversion [67–69]. Alternatively, PrP^C downregulation has also been proposed to treat prion diseases [70, 71]. In light of our results, restoring NMDAR modulation may block the progression of excitotoxicity and ensuing neuronal loss. A promising possibility is given by a new class of drugs, named NitroMemantines, which combines memantine with a NO-generating group [72, 73]. Memantine is a Food and Drug Administration-approved drug for the treatment of Alzheimer disease and acts by blocking NMDAR-prolonged activation [74, 75]. In NitroMemantine, a NO group is added to target NMDAR nitrosylation sites. NitroMemantine mechanism of action may therefore replace the protective NMDAR S-nitrosylation we found impaired in prion disorders [33].

Methods

Ethic Statement

Animals were obtained from Charles River Laboratory and housed at the animal facility of IRCCS Foundation “Carlo Besta” Neurological Institute, Milan, Italy. CD1 female mice were housed in groups of two to five animals in individually ventilated cages in a room with controlled 12:12 light/dark cycle and with food and water ad libitum. Regular veterinary care was performed for assessment of animal health. Animal facility is licensed and inspected by the Italian Ministry of Health. Experimental procedures were performed in

accordance with European regulations (Directive 2010/63/EU) and with Italian Legislative Decree 26/2014 and were approved by the local authority veterinary service and by the Italian Ministry of Health, Directorate General for Animal Health. All efforts were made to minimize animal suffering and to reduce the number of animals used.

Animal Groups

Sixty CD1 female mice were used in this study. Thirty animals were divided in three groups of ten mice. Each group was inoculated with a different mouse-adapted scrapie strain: RML, 139A, and ME7. Brain samples were collected at different timepoints. Five animals for each group were sacrificed 30 dpi at pre-symptomatic phase of the disease. The remaining mice were monitored and sacrificed at the terminal stage of the disease, which is characterized by superficial breathing and lateral decubitus. Thirty control mice were not injected with infected brain homogenate, and brain samples were collected at ages corresponding to pre-symptomatic and terminal stage of infected mice.

Intracerebral Inoculation

Two-month-old CD1 mice were anesthetized with intraperitoneal administration of tribromoethanol (100 μL/10 g) and stereotaxically inoculated in the striatum (using these coordinates: − 0.5 caudal, + 2 lateral, + 3.5 depth) with 20 μL of 10% *w/v* brain homogenates from terminally ill animals infected with RML, ME7, or 139A scrapie strains. All surgical procedures were performed under sterile conditions.

Sacrifice

Animals were deeply anesthetized by intraperitoneal injection of tribromoethanol. Transcardial perfusion with phosphate-buffered saline (PBS) + 5-mM EDTA was performed, and the brains were removed. Two hemibrains for each group of five animals were processed for histological analysis. From the two remaining hemibrains and from the other three whole samples, hippocampi were dissected, immediately frozen in liquid nitrogen, and stored at − 80 °C to be processed for biochemical measurements. Hippocampi derived from the same mouse were always addressed to different biochemical analysis (biotin switch assay or SNOB1). For each biochemical method, four hippocampi were used at most. PK digestion was performed by using exceeding hippocampal homogenates from biotin switch assay.

Histological Staining

Hemibrains were fixed in Alcolin (Diapath), dehydrated, and embedded in paraplast. Seven-micrometer-thick serial sections were stained with H&E or immunostained with monoclonal antibodies to PrP (6H4, Prionics). Before PrP immunostaining, the sections were sequentially treated with 10 μg/mL of PK for 5 min and with 3-M guanidine isothiocyanate for 20 min. Non-specific binding was prevented using ARK kit (Dako), and immunoreactions were visualized using 3-3′-diaminobenzidine (DAB, Dako) as chromogen.

PK Digestion

Fifty micrograms of proteins from control and infected hippocampal homogenates prepared in HEN buffer (see "Protein S-Nitrosylation Detection by Biotin Switch Assay" paragraph) were digested with 50 μg/mL of PK for 1 h at 37 °C. Thirty micrograms of protein extract was loaded as input without PK digestion. After addition of sample buffer, samples were boiled for 10 min at 95 °C and processed for SDS-PAGE and Western blot detection of PrP.

Protein S-Nitrosylation Detection by Biotin Switch Assay

To compare GluN2A and GluN1 S-nitrosylation levels in control and infected samples, the biotin switch assay was performed as previously described [30]. Briefly, one control and one infected hippocampus (age-matched samples at pre-symptomatic or terminal stage of the disease) were separately homogenized in 400-μL HEN buffer: 250-mM HEPES pH 7.5 (H3375, Sigma-Aldrich), 1-mM EDTA (E6758, Sigma-Aldrich), 0.1-mM neocuproine (N1501, Sigma-Aldrich), and protease inhibitor cocktail (Roche Diagnostics Corp.). Homogenates were cleared by centrifugation at 2000 *g*, 10 min at 4 °C. Bicinchoninic acid assay was performed to determine protein concentration in the supernatant. One milligram of proteins was diluted to 0.8 μg/μL in HEN buffer + 0.04% CHAPS (C9426, Sigma-Aldrich) and incubated at 50 °C for 1 h in 4 volumes of blocking solution: 9 volumes of HEN, 1 volume of 25% *w/v* SDS (L3771, Sigma-Aldrich) in ddH2O, and 20-mM S-methyl thiomethanesulfonate (64306, Sigma-Aldrich) from the 2-M stock solution in dimethylformamide. S-Methyl thiomethanesulfonate was removed by acetone precipitation, and the pellet was resuspended in 100 μL of HENS buffer (HEN + 1% SDS) per mg of starting proteins. Ascorbate (A4034, Sigma-Aldrich), prepared as 180 mM in ddH2O, was added to 30-mM final concentration in the samples and incubated for 3 h at 25 °C to selectively reduce S-nitrosylated thiols. The efficiency of thiols blocking was checked by performing a negative control without ascorbate on control samples. Ascorbate was removed by acetone precipitation, and the protein pellet was resuspended in 100 μL of HENS buffer per mg of starting proteins. Free thiols were bound to EZ-Link HPDP-biotin (21341, Thermo Scientific), which was added 1:3 to the samples from the 4-

mM stock in dimethylformamide. The selective binding to the resin was checked by performing a negative control without biotin on control samples. After 1-h incubation at 25 °C, HPDP-biotin was removed by dialysis in HENS buffer. Biotinylated proteins were purified by adding to the samples 2 volumes of neutralization buffer (20-mM HEPES pH 7.5, 100-mM NaCl, 1-mM EDTA, 0.5% Triton X-100) and 50 μL of wet immobilized NeutrAvidin agarose resin (29200, Thermo Scientific) and incubating for 2 h at room temperature (RT). After resin washing for five times with neutralization buffer adjusted to 600-mM NaCl, biotinylated proteins were eluted in a sample buffer, boiled, and processed for SDS-PAGE and Western blot detection of GluN1, GluN2A, and β-actin. For each sample, 30 μg of protein extract was loaded as input. S-Nitrosylation signals were normalized on the corresponding input and on β-actin value by applying the following formula: (NMDAR subunit S-nitrosylation/input)/(β-actin S-nitrosylation/input).

Protein S-Nitrosylation Detection by SNOB1 Reagent

To compare GluN2A and GluN1 S-nitrosylation levels in control and infected hippocampi, the SNOB1 reagent (sc-361363, Santa Cruz Biotechnology) was used as previously described [30]. One control and one infected hippocampus were separately homogenized in 500-μL PBS + 0.5% Triton X-100 + protease inhibitors and centrifuged 10 min at 5000 rpm at 4 °C. After protein concentration determination, the same amount of protein was used and PBS + 0.5% Triton was added up to 1 mL. Samples were incubated with 0.5-mM SNOB1 for 30 min at 37 °C in the dark, according to the manufacturer's instructions. A negative control was performed incubating the control sample with 0.5-mM biotin for 30 min at 37 °C in the dark. To purify SNOB1-bound proteins, 50 μL of wet immobilized NeutrAvidin agarose resin was added to the samples and incubated for 2 h at RT. Resin was washed five times with PBS + 0.5% Triton. Then, proteins were eluted in sample buffer, boiled, and processed for SDS-PAGE and Western blot detection of GluN1, GluN2A, and β-actin. For each sample, 30 μg of protein extract was loaded as input. S-Nitrosylation signals were normalized on the corresponding input and on β-actin value by applying the following formula: (SNOB1-NMDAR subunit / input) / (SNOB1-β-actin / input).

SDS-PAGE and Western Blot

Proteins in sample buffer (10% glycerol, 50-mM Tris-HCl pH 6.8, 2% *w/v* SDS, 4-M urea, 0.005% bromophenol blue) were boiled and separated by SDS-PAGE in 8–12% polyacrylamide gels. Proteins were transferred on nitrocellulose, and after 1 h in blocking solution, membranes were incubated overnight at 4 °C with the following primary antibodies: anti-GluN1 1:500 (G8913, Sigma-Aldrich); anti-GluN2A 1:500 (G9038, Sigma-Aldrich); anti-β-actin peroxidase (AC-15) 1:10000 (A3854, Sigma-Aldrich); and anti-PrP W226 (kindly provided by PD Dr. Michael Knittler, Institute of Immunology Friedrich-Loeffler-Institute, Greifswald-Insel Riems, Germany). After incubation with the secondary antibody, membranes were developed with ECL detection reagent (GE Healthcare) and recorded by the digital imaging system Alliance 4.7 (UVITEC). Band quantification was performed with Uviband 15.0 software (UVITEC), obtaining an optical density value.

Statistical Analysis

Control and infected samples were compared by performing the Student's *t* test, setting two-tailed distribution and two-sample unequal variance. $p < 0.05$ was considered statistically significant.

Funding Information This work was supported/partially supported by the Italian Ministry of Health (GR-2013-02355724 and RC) to FM, Italian Ministry of Health to FT, SISSA Intramural Funding to GL, and SISSA grant to FB (Young SISSA Scientists Research Projects 2011–2012 Scheme). The funders had no role in study design, data collection and analysis, decision to publish, or preparation of the manuscript.

Compliance with Ethical Standards

Animal procedures were performed in accordance with European regulations (Directive 2010/63/EU) and with Italian Legislative Decree 26/2014 and were approved by the local authority veterinary service and by the Italian Ministry of Health, Directorate General for Animal Health. All efforts were made to minimize animal suffering and to reduce the number of animals used. Animal facility is licensed and inspected by the Italian Ministry of Health.

Conflict of Interests The authors declare that they have no competing interests.

References

1. Prusiner SB (2001) Neurodegenerative diseases and prions. N Engl J Med 344(20):1516–1526. https://doi.org/10.1056/NEJM200105173442006
2. Aguzzi A, Heikenwalder M, Miele G (2004) Progress and problems in the biology, diagnostics, and therapeutics of prion diseases. J Clin Invest 114(2):153–160. https://doi.org/10.1172/JCI22438
3. Prusiner SB (1982) Novel proteinaceous infectious particles cause scrapie. Science 216(4542):136–144
4. Oesch B, Westaway D, Walchli M, McKinley MP, Kent SB, Aebersold R, Barry RA, Tempst P, Teplow DB, Hood LE, et al. (1985) A cellular gene encodes scrapie PrP 27-30 protein. Cell 40 (4):735–746.
5. Caughey BW, Dong A, Bhat KS, Ernst D, Hayes SF, Caughey WS (1991) Secondary structure analysis of the scrapie-associated

protein PrP 27-30 in water by infrared spectroscopy. Biochemistry 30(31):7672–7680
6. Gasset M, Baldwin MA, Fletterick RJ, Prusiner SB (1993) Perturbation of the secondary structure of the scrapie prion protein under conditions that alter infectivity. Proc Natl Acad Sci U S A 90(1):1–5
7. Bieschke J, Weber P, Sarafoff N, Beekes M, Giese A, Kretzschmar H (2004) Autocatalytic self-propagation of misfolded prion protein. Proc Natl Acad Sci U S A 101(33):12207–12211. https://doi.org/10.1073/pnas.0404650101
8. Soto C (2003) Unfolding the role of protein misfolding in neurodegenerative diseases. Nat Rev Neurosci 4(1):49–60. https://doi.org/10.1038/nrn1007
9. Soto C, Satani N (2011) The intricate mechanisms of neurodegeneration in prion diseases. Trends Mol Med 17(1):14–24. https://doi.org/10.1016/j.molmed.2010.09.001
10. Budka H (2003) Neuropathology of prion diseases. Br Med Bull 66:121–130
11. Westergard L, Christensen HM, Harris DA (2007) The cellular prion protein (PrP(C)): its physiological function and role in disease. Biochim Biophys Acta 1772(6):629–644. https://doi.org/10.1016/j.bbadis.2007.02.011
12. Halliday M, Radford H, Mallucci GR (2014) Prions: generation and spread versus neurotoxicity. J Biol Chem 289(29):19862–19868. https://doi.org/10.1074/jbc.R114.568477
13. Brown DR (2001) Prion and prejudice: normal protein and the synapse. Trends Neurosci 24(2):85–90
14. Aguzzi A, Baumann F, Bremer J (2008) The prion's elusive reason for being. Annu Rev Neurosci 31:439–477. https://doi.org/10.1146/annurev.neuro.31.060407.125620
15. Caughey B, Baron GS (2006) Prions and their partners in crime. Nature 443(7113):803–810. https://doi.org/10.1038/nature05294
16. Collinge J, Whittington MA, Sidle KC, Smith CJ, Palmer MS, Clarke AR, Jefferys JG (1994) Prion protein is necessary for normal synaptic function. Nature 370(6487):295–297. https://doi.org/10.1038/370295a0
17. Manson JC, Hope J, Clarke AR, Johnston A, Black C, MacLeod N (1995) PrP gene dosage and long term potentiation. Neurodegeneration 4(1):113–114
18. Colling SB, Collinge J, Jefferys JG (1996) Hippocampal slices from prion protein null mice: disrupted Ca(2+)-activated K+ currents. Neurosci Lett 209(1):49–52
19. Carleton A, Tremblay P, Vincent JD, Lledo PM (2001) Dose-dependent, prion protein (PrP)-mediated facilitation of excitatory synaptic transmission in the mouse hippocampus. Pflugers Arch 442(2):223–229
20. Herms JW, Tings T, Dunker S, Kretzschmar HA (2001) Prion protein affects Ca^{2+}-activated K^+ currents in cerebellar Purkinje cells. Neurobiol Dis 8(2):324–330. https://doi.org/10.1006/nbdi.2000.0369
21. Mallucci GR, Ratte S, Asante EA, Linehan J, Gowland I, Jefferys JG, Collinge J (2002) Post-natal knockout of prion protein alters hippocampal CA1 properties, but does not result in neurodegeneration. EMBO J 21(3):202–210. https://doi.org/10.1093/emboj/21.3.202
22. Maglio LE, Perez MF, Martins VR, Brentani RR, Ramirez OA (2004) Hippocampal synaptic plasticity in mice devoid of cellular prion protein. Brain Res Mol Brain Res 131(1–2):58–64. https://doi.org/10.1016/j.molbrainres.2004.08.004
23. Fuhrmann M, Bittner T, Mitteregger G, Haider N, Moosmang S, Kretzschmar H, Herms J (2006) Loss of the cellular prion protein affects the Ca^{2+} homeostasis in hippocampal CA1 neurons. J Neurochem 98(6):1876–1885. https://doi.org/10.1111/j.1471-4159.2006.04011.x
24. Prestori F, Rossi P, Bearzatto B, Laine J, Necchi D, Diwakar S, Schiffmann SN, Axelrad H, D'Angelo E (2008) Altered neuron excitability and synaptic plasticity in the cerebellar granular layer of juvenile prion protein knock-out mice with impaired motor control. J Neurosci 28 (28):7091–7103. doi:https://doi.org/10.1523/JNEUROSCI.0409-08.2008
25. Lazzari C, Peggion C, Stella R, Massimino ML, Lim D, Bertoli A, Sorgato MC (2011) Cellular prion protein is implicated in the regulation of local Ca^{2+} movements in cerebellar granule neurons. J Neurochem 116(5):881–890. https://doi.org/10.1111/j.1471-4159.2010.07015.x
26. Khosravani H, Zhang Y, Tsutsui S, Hameed S, Altier C, Hamid J, Chen L, Villemaire M et al (2008) Prion protein attenuates excitotoxicity by inhibiting NMDA receptors. J Cell Biol 181(3):551–565. https://doi.org/10.1083/jcb.200711002
27. You H, Tsutsui S, Hameed S, Kannanayakal TJ, Chen L, Xia P, Engbers JD, Lipton SA et al (2012) Abeta neurotoxicity depends on interactions between copper ions, prion protein, and N-methyl-D-aspartate receptors. Proc Natl Acad Sci U S A 109(5):1737–1742. https://doi.org/10.1073/pnas.1110789109
28. Spudich A, Frigg R, Kilic E, Kilic U, Oesch B, Raeber A, Bassetti CL, Hermann DM (2005) Aggravation of ischemic brain injury by prion protein deficiency: role of ERK-1/-2 and STAT-1. Neurobiol Dis 20 (2):442–449. doi:10.1016/j.nbd.2005.04.002
29. Rangel A, Burgaya F, Gavin R, Soriano E, Aguzzi A, Del Rio JA (2007) Enhanced susceptibility of Prnp-deficient mice to kainate-induced seizures, neuronal apoptosis, and death: role of AMPA/kainate receptors. J Neurosci Res 85(12):2741–2755. https://doi.org/10.1002/jnr.21215
30. Gasperini L, Meneghetti E, Pastore B, Benetti F, Legname G (2015) Prion protein and copper cooperatively protect neurons by modulating NMDA receptor through S-nitrosylation. Antioxid Redox Signal 22(9):772–784. https://doi.org/10.1089/ars.2014.6032
31. Choi YB, Tenneti L, Le DA, Ortiz J, Bai G, Chen HS, Lipton SA (2000) Molecular basis of NMDA receptor-coupled ion channel modulation by S-nitrosylation. Nat Neurosci 3(1):15–21. https://doi.org/10.1038/71090
32. Lipton SA, Choi YB, Takahashi H, Zhang D, Li W, Godzik A, Bankston LA (2002) Cysteine regulation of protein function—as exemplified by NMDA-receptor modulation. Trends Neurosci 25(9):474–480
33. Nakamura T, Lipton SA (2011) Redox modulation by S-nitrosylation contributes to protein misfolding, mitochondrial dynamics, and neuronal synaptic damage in neurodegenerative diseases. Cell Death Differ 18(9):1478–1486. https://doi.org/10.1038/cdd.2011.65
34. Kone BC, Kuncewicz T, Zhang W, Yu ZY (2003) Protein interactions with nitric oxide synthases: controlling the right time, the right place, and the right amount of nitric oxide. American Journal of Physiology Renal Physiology 285(2):F178–F190. https://doi.org/10.1152/ajprenal.00048.2003
35. Forstermann U, Sessa WC (2012) Nitric oxide synthases: regulation and function. European Heart Journal 33(7):829–837, 837a-837d. https://doi.org/10.1093/eurheartj/ehr304
36. Delint-Ramirez I, Fernandez E, Bayes A, Kicsi E, Komiyama NH, Grant SG (2010) In vivo composition of NMDA receptor signaling complexes differs between membrane subdomains and is modulated by PSD-95 and PSD-93. J Neurosci 30(24):8162–8170. https://doi.org/10.1523/jneurosci.1792-10.2010
37. Naslavsky N, Stein R, Yanai A, Friedlander G, Taraboulos A (1997) Characterization of detergent-insoluble complexes containing the cellular prion protein and its scrapie isoform. J Biol Chem 272(10):6324–6331
38. Bonomo RP, Pappalardo G, Rizzarelli E, Tabbi G, Vagliasindi LI (2008) Studies of nitric oxide interaction with mono- and dinuclear copper(II) complexes of prion protein bis-octarepeat fragments. Dalton Trans (29):3805–3816. https://doi.org/10.1039/B719930A
39. Stockel J, Safar J, Wallace AC, Cohen FE, Prusiner SB (1998) Prion protein selectively binds copper(II) ions.

Biochemistry 37(20):7185–7193. https://doi.org/10.1021/bi972827kbi972827k[pii]
40. Jackson GS, Murray I, Hosszu LL, Gibbs N, Waltho JP, Clarke AR, Collinge J (2001) Location and properties of metal-binding sites on the human prion protein. Proc Natl Acad Sci USA 98(15):8531–8535. https://doi.org/10.1073/pnas.151038498151038498[pii]
41. Singh N, Das D, Singh A, Mohan ML (2010) Prion protein and metal interaction: physiological and pathological implications. Curr Issues Mol Biol 12(2):99–107
42. Liu L, Jiang D, McDonald A, Hao Y, Millhauser GL, Zhou F (2011) Copper redox cycling in the prion protein depends critically on binding mode. J Am Chem Soc 133(31):12229–12237. https://doi.org/10.1021/ja2045259
43. Benvegnu S, Poggiolini I, Legname G (2010) Neurodevelopmental expression and localization of the cellular prion protein in the central nervous system of the mouse. J Comp Neurol 518(11):1879–1891. https://doi.org/10.1002/cne.22357
44. Marmiroli P, Cavaletti G (2012) The glutamatergic neurotransmission in the central nervous system. Curr Med Chem 19(9):1269–1276
45. Prusiner SB, Groth DF, Bolton DC, Kent SB, Hood LE (1984) Purification and structural studies of a major scrapie prion protein. Cell 38(1):127–134
46. Chiesa R, Harris DA (2001) Prion diseases: what is the neurotoxic molecule? Neurobiol Dis 8(5):743–763. https://doi.org/10.1006/nbdi.2001.0433
47. Bueler H, Fischer M, Lang Y, Bluethmann H, Lipp HP, DeArmond SJ, Prusiner SB, Aguet M et al (1992) Normal development and behaviour of mice lacking the neuronal cell-surface PrP protein. Nature 356(6370):577–582. https://doi.org/10.1038/356577a0
48. Manson JC, Clarke AR, Hooper ML, Aitchison L, McConnell I, Hope J (1994) 129/Ola mice carrying a null mutation in PrP that abolishes mRNA production are developmentally normal. Mol Neurobiol 8(2–3):121–127. https://doi.org/10.1007/BF02780662
49. Steele AD, Lindquist S, Aguzzi A (2007) The prion protein knockout mouse: a phenotype under challenge. Prion 1(2):83–93
50. Chiesa R, Harris DA (2009) Fishing for prion protein function. PLoS Biol 7(3):e75. https://doi.org/10.1371/journal.pbio.1000075
51. Linden R, Martins VR, Prado MA, Cammarota M, Izquierdo I, Brentani RR (2008) Physiology of the prion protein. Physiol Rev 88(2):673–728. https://doi.org/10.1152/physrev.00007.2007
52. Lewerenz J, Maher P (2015) Chronic glutamate toxicity in neurodegenerative diseases—what is the evidence? Front Neurosci 9:469. https://doi.org/10.3389/fnins.2015.00469
53. Telling GC, Parchi P, DeArmond SJ, Cortelli P, Montagna P, Gabizon R, Mastrianni J, Lugaresi E et al (1996) Evidence for the conformation of the pathologic isoform of the prion protein enciphering and propagating prion diversity. Science 274(5295):2079–2082
54. Solforosi L, Milani M, Mancini N, Clementi M, Burioni R (2013) A closer look at prion strains: characterization and important implications. Prion 7(2):99–108. https://doi.org/10.4161/pri.23490
55. Jendroska K, Heinzel FP, Torchia M, Stowring L, Kretzschmar HA, Kon A, Stern A, Prusiner SB et al (1991) Proteinase-resistant prion protein accumulation in Syrian hamster brain correlates with regional pathology and scrapie infectivity. Neurology 41(9):1482–1490
56. Williams A, Lucassen PJ, Ritchie D, Bruce M (1997) PrP deposition, microglial activation, and neuronal apoptosis in murine scrapie. Exp Neurol 144(2):433–438. https://doi.org/10.1006/exnr.1997.6424
57. Jeffrey M, Martin S, Barr J, Chong A, Fraser JR (2001) Onset of accumulation of PrPres in murine ME7 scrapie in relation to pathological and PrP immunohistochemical changes. J Comp Pathol 124(1):20–28. https://doi.org/10.1053/jcpa.2000.0423
58. Hill AF, Collinge J (2003) Subclinical prion infection in humans and animals. Br Med Bull 66(1):161–170. https://doi.org/10.1093/bmb/66.1.161
59. Bueler H, Aguzzi A, Sailer A, Greiner RA, Autenried P, Aguet M, Weissmann C (1993) Mice devoid of PrP are resistant to scrapie. Cell 73(7):1339–1347
60. Sonati T, Reimann RR, Falsig J, Baral PK, O'Connor T, Hornemann S, Yaganoglu S, Li B et al (2013) The toxicity of antiprion antibodies is mediated by the flexible tail of the prion protein. Nature 501(7465):102–106. https://doi.org/10.1038/nature12402
61. Resenberger UK, Harmeier A, Woerner AC, Goodman JL, Muller V, Krishnan R, Vabulas RM, Kretzschmar HA et al (2011) The cellular prion protein mediates neurotoxic signalling of beta-sheet-rich conformers independent of prion replication. EMBO J 30(10):2057–2070. https://doi.org/10.1038/emboj.2011.86
62. Muller WE, Ushijima H, Schroder HC, Forrest JM, Schatton WF, Rytik PG, Heffner-Lauc M (1993) Cytoprotective effect of NMDA receptor antagonists on prion protein (PrionSc)-induced toxicity in rat cortical cell cultures. Eur J Pharmacol 246(3):261–267
63. Singh N, Singh A, Das D, Mohan ML (2010) Redox control of prion and disease pathogenesis. Antioxid Redox Signal 12(11):1271–1294. https://doi.org/10.1089/ars.2009.2628
64. Petersen RB, Siedlak SL, Lee H-g, Kim Y-S, Nunomura A, Tagliavini F, Ghetti B, Cras P et al (2005) Redox metals and oxidative abnormalities in human prion diseases. Acta Neuropathol 110(3):232–238. https://doi.org/10.1007/s00401-005-1034-4
65. Chen LN, Sun J, Yang XD, Xiao K, Lv Y, Zhang BY, Zhou W, Chen C et al (2016) The brain NO levels and NOS activities ascended in the early and middle stages and descended in the terminal stage in scrapie-infected animal models. Mol Neurobiol 54:1786–1796. https://doi.org/10.1007/s12035-016-9755-z
66. Ju WK, Park KJ, Choi EK, Kim J, Carp RI, Wisniewski HM, Kim YS (1998) Expression of inducible nitric oxide synthase in the brains of scrapie-infected mice. J Neurovirol 4(4):445–450
67. Cashman NR, Caughey B (2004) Prion diseases—close to effective therapy? Nat Rev Drug Discov 3(10):874–884. https://doi.org/10.1038/nrd1525
68. Rigter A, Langeveld JP, van Zijderveld FG, Bossers A (2010) Prion protein self-interactions: a gateway to novel therapeutic strategies? Vaccine 28(49):7810–7823. https://doi.org/10.1016/j.vaccine.2010.09.012
69. Aguzzi A, O'Connor T (2010) Protein aggregation diseases: pathogenicity and therapeutic perspectives. Nat Rev Drug Discov 9(3):237–248. https://doi.org/10.1038/nrd3050
70. Mallucci G, Dickinson A, Linehan J, Klohn PC, Brandner S, Collinge J (2003) Depleting neuronal PrP in prion infection prevents disease and reverses spongiosis. Science 302(5646):871–874. https://doi.org/10.1126/science.1090187302/5646/871[pii]
71. Pfeifer A, Eigenbrod S, Al-Khadra S, Hofmann A, Mitteregger G, Moser M, Bertsch U, Kretzschmar H (2006) Lentivector-mediated RNAi efficiently suppresses prion protein and prolongs survival of scrapie-infected mice. J Clin Invest 116(12):3204–3210. https://doi.org/10.1172/jci29236
72. Lipton SA (2006) Paradigm shift in neuroprotection by NMDA receptor blockade: memantine and beyond. Nat Rev Drug Discov 5(2):160–170
73. Lipton SA (2007) Pathologically activated therapeutics for neuroprotection. Nat Rev Neurosci 8(10):803–808. https://doi.org/10.1038/nrn2229
74. Okamoto S, Pouladi MA, Talantova M, Yao D, Xia P, Ehrnhoefer DE, Zaidi R, Clemente A et al (2009) Balance between synaptic versus extrasynaptic NMDA receptor activity influences inclusions and neurotoxicity of mutant huntingtin. Nat Med 15(12):1407–1413. https://doi.org/10.1038/nm.2056
75. Chen HS, Pellegrini JW, Aggarwal SK, Lei SZ, Warach S, Jensen FE, Lipton SA (1992) Open-channel block of N-methyl-D-aspartate (NMDA) responses by memantine: therapeutic advantage against NMDA receptor-mediated neurotoxicity. J Neurosci 12(11):4427–4436